Journal of
Nanoscience and Nanotechnology
Vol. 13, 6424–6428, 2013

RESEARCH ARTICLE

An Electrochemical H_2O_2 Detection Method Based on Direct Electrochemistry of Myoglobin Immobilized on Gold Deposited ITO Electrode

Santosh Machhindra Dengale[1], Ajay Kumar Yagati[2], Yong-Ho Chung[2], Junhong Min[3], and Jeong-Woo Choi[1, 2, *]

[1] *Interdisciplinary Program of Integrated Biotechnology, Sogang University, 35 Baekbeom-ro, Mapo-gu, Seoul 121-742, Republic of Korea*
[2] *Department of Chemical and Biomolecular Engineering, Sogang University, 35 Baekbeom-ro, Mapo-gu, Seoul 121-742, Republic of Korea*
[3] *School of Integrative Engineering, Chung-Ang University, Heukseok-dong, Dongjak-gu, Seoul 156-756, Republic of Korea*

A protein based electrochemical sensor for the detection of hydrogen peroxide based on Myoglobin immobilized on gold nano structures patterned on Indium tin oxide electrode was developed. A uniformly distributed nanometer sized Au-array on ITO electrode surface was obtained by optimizing electro deposition conditions. The morphology of Mb molecules and Au-nanostructures on ITO was investigated by scanning electron microscopy. A Cyclic voltammetry technique was employed to study electrochemical behavior of immobilized Mb on Au/ITO electrode. From CV, a pair of quasi-reversible redox peaks of Mb obtained in 10 mM PBS buffer solution at 0.28 and 0.11 V respectively. From the electrochemical experiments, it is observed that Mb/Au/ITO electrode provides a facile electron transfer between Mb and modified ITO electrode and it also catalyzes the reduction of H_2O_2. A linear increase in amperometric current with increase in H_2O_2 concentration was also observed. The stability, reusability and selectivity of the biosensor were also evaluated. The proposed biosensor exhibits an effective and fast catalytic response to reduction of H_2O_2 which can be used in future biosensor applications.

Keywords: Biosensor, Amperometric, Myoglobin, Electrodeposition, Cyclic Voltammetry.

1. INTRODUCTION

H_2O_2 is an important intermediate product of vital reactions, and it is useful to study hydrogen peroxide (H_2O_2) on life processes. Therefore, it is particularly important to detect H_2O_2 and its detection attracts the attention of many investigators.[1] The fast electrochemical H_2O_2 sensing with selectivity and sensitivity has emerged an analytical tool because its role as an essential mediator in food, pharmaceutical, clinical, industrial and environmental analyses.[2–3] Also H_2O_2 is the main product of most enzymatic reactions; thus, its detection is very interesting for the development of biosensors.[4,5] Hence several analytical methods have been developed for the detection of H_2O_2, such as fluorescence, chemiluminescence, and electrochemical methods.[6–8] Among these methods, electrochemical detection of H_2O_2 has advantages like low detection limit and low costs. Many electrochemical techniques make use of the reduction of H_2O_2 by the catalysis of immobilized enzymes or protein to construct biosensors, which are based on direct electron transfer between an electrode and immobilized protein.[9–13] It is also well known that the study of direct electron transfer of redox proteins can establish a good model for understanding the complicated electron transfer mechanisms in biological systems and elucidating the relationship between their structures and biological functions.[14] However, direct electron transfer between redox proteins and electrode is usually sluggish due to the deep burying of electroactive groups in the protein, denaturing caused by the serious adsorption of proteins at the electrode surface, and the unfavorable orientation of the protein immobilized at the electrode surface.[15]

When a redox protein is immobilized on biocompatible metal nanostructures, it will exhibit reasonably fast electron transfer kinetics and permit the electrochemical

*Author to whom correspondence should be addressed.

1533-4880/2013/13/6424/005 doi:10.1166/jnn.2013.7618

measurement of its substrate without addition of a mediator to the analyzed solution.[16] Gold nanoparticles (AuNPs), including the AuNP-modified electrodes have been extensively used for different applications.[17–19] AuNP-modified electrodes can be prepared by potential-step or pulse-potential electrodeposition and the control of particle density and size distribution achieved by adjusting the electrodeposition parameters was discussed. Apparently, the good biocompatibility and abundant edge sites of the AuNP/ITO electrode offer great advantages for the fabrication of biosensors. Metal nanoparticles in conjugation with redox proteins have been proved good candidates for enzymatic molecule based biosensors as AuNPs has large surface area for enzyme immobilization, its biocompatible nature and suitable for direct electron transfer from catalytic molecule to electrode.[20] Hence the modified hybrid electrodes usually exhibit a unique electrocatalytic behavior or high sensitivity. The electrochemical detection of H_2O_2 by using protein containing the heme groups, such as myoglobin[21–22] and hemoglobin[23–24] which possess peroxidase like catalytic activity, which can reduce H_2O_2 due to electroactive heme center, has been reported by different research groups.

Myoglobin (Mb) is a 16.7 kDa heme protein in muscle tissues which functions to store and transport oxygen. It contains a single polypeptide chain with an iron heme as its prosthetic group. Studies of electrochemical behavior of heme proteins are essential for a fundamental understanding of their biological activity.[25] Mb is an ideal molecule for the study of electron-transfer reactions of heme proteins and also for biosensing and electrocatalysis. Owing to the commercial availability and known structure, myoglobin (Mb) was used as an ideal model protein for catalytic reduction of H_2O_2 in this work. In this paper, the Mb immobilized on gold nanoparticles formed on ITO surface, showed fast direct electron transfer and excellent electrocatalytic activity to the reduction of hydrogen peroxide, leading to good analytical performance for electrochemical detection of hydrogen peroxide.

2. EXPERIMENTAL DETAILS

2.1. Materials and Reagents

Myoglobin from horse heart was purchased from Sigma-Aldrich (St. Louis, MO., USA) was used as received and stored at −20 °C. Hydrogen tetracloroaurate trihydrate ($HAuCl_4 \cdot 3H_2O$), 11-mercaptoundecanoic acid (MUA), *N*-hydroxysuccinimide (NHS), 1-ethyl-3-(3-diethylaminopropyl) carbodiimide hydrochloride (EDC) and isopropyl alcohol were also obtained from Sigma-Aldrich. Polyethylene glycol (PEG-200) from Yakuri Chemicals (Japan) was used as received. Hydrogen Peroxide (H_2O_2) (30%) was brought form Daejung materials and chemicals (South Korea) and diluted in DI water to prepare different concentration solutions. The electrolyte for CV experiments is 10 mM phosphate buffered saline (PBS) of pH 7.0. All other chemicals were of reagent grade and used as received. All solutions were prepared with pure water (18 MΩ cm) purified with a Milli-Q system (Millipore, Bedford, MA). All electrochemical experiments were performed in 10 mM PBS buffer solution with pH 7.0. High purity nitrogen was used for deaeration. The buffer and sample solutions were purged with highly purified nitrogen for 5 min prior to each experiment. Nitrogen atmosphere was maintained over the solutions during experiments.

2.2. Preparation and Modification of Au-ITO Surface

Indium tin oxide [ITO; 20 Ω/cm^2] of a 400 nm thickness was used in all experiments. The transparent electrodes were cleaned by ultrasonic cleaning in solutions of Triton X-100/water, water, and ethanol for 40 min each successively. The ITO electrode was then subjected to base piranha solution treatment in a solution of $NH_4OH:H_2O_2:H_2O$ (1:1:5) for 40 min at 80 °C, rinsed thoroughly with water, and dried under a stream of nitrogen gas for generation of –OH groups on the ITO surface. The cleaned ITO was immersed in 1.2 mM $HAuCl_4$ and PEG electrolyte. The gold nanostructure was electrodeposited in 1.2 mM $HAuCl_4$, at step potentials, −1.8, −1.3 and −0.13 V for 75 s. Traces of adsorbed PEG on AuNPs were removed by keeping the AuNP/ITO electrode in boiling isopropyl alcohol for 3 minutes.

For the formation of Mb/AuNPs/ITO electrode, Au-electrodeposited ITO was incubated with 20 mM 11-MUA and later with EDC and NHS.[26–27] 20 μL of 0.20 mg/ml Mb was dropped on this activated electrode surface and kept in refrigerator at 4 °C for 24-hours before using it for electrochemical study. To remove unbound protein molecules, Mb/AuNPs/ITO were thoroughly washed with DI water and dried with N_2 gas. The immobilization process of myoglobin on AuNP/ITO is represented in Figure 1.

2.3. Apparatus and Measurements

UV-Vis absorbance spectroscopy was performed using a UV-Vis-3100-Nir Recording Spectrophotometer (Shimadzu, Japan). Scanning electron microscopy images were obtained using a field emission scanning electron microscope (Hitachi S-4300) operation at an acceleration

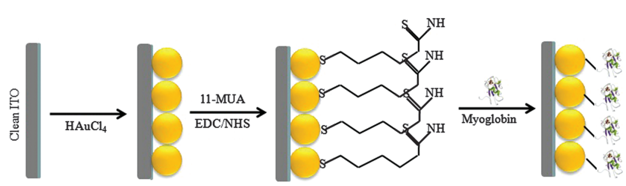

Fig. 1. Schematic diagram for stepwise electrode modification for the formation of Mb/AuNPs/ITO electrode surface.

RESEARCH ARTICLE

voltage of 20 kV. Electrochemical measurements were performed on a CHI 730 A electrochemical analyzer (CHI Co.) at room temperature (25 °C) with a conventional three-electrode system with Mb/AuNPs/ITO as a working electrode, a platinum wire as an auxiliary electrode, and $Ag/AgCl/KCl_{sat.}$ as a reference electrode. For cyclic voltammetry experiments of Mb/Au/ITO electrode, the scanning potential range was set from 0.5 V to 0.0 V at the scan rate 100 mV s^{-1}. The current-time measurements were carried out at 0.5 mV with successive addition of 10 μL of 100 mM H_2O_2 in 10 ml of 10 mM PBS buffer electrolyte, pH 7.0.

3. RESULTS AND DISCUSSION

3.1. Surface Morphology of the Au Electrodeposited ITO Electrode

Electrochemical deposition could provide an easy and rapid alternative for the preparation of gold nanoparticles electrodes in a short time. The SEM was used to evaluate the physical appearance and surface characteristics of AuNPs on electrode surfaces. The SEM morphologies of the AuNP/ITO surfaces are shown in Figure 2. As can be seen, many spherical gold nanoparticles are electrodeposited on the ITO film coated glass surface (Figs. 2(a), (b)). As deposition potential is increased from −0.13 to −1.8 V, the number of particles increases.[25] Bumpy particles are formed at potential −0.13 V. The potential dependence of nanoparticle density and size has been described elsewhere.[31] The higher negative overpotential is responsible for the formation of more number of nucleation centers and these nucleation centers grows into particles with time. If the numbers of such nucleation sites are more, then the metal ions from electrolyte will be utilized to increase the nuclei size rather than forming a particle on bare ITO. This also results both in the particle size increase as well as

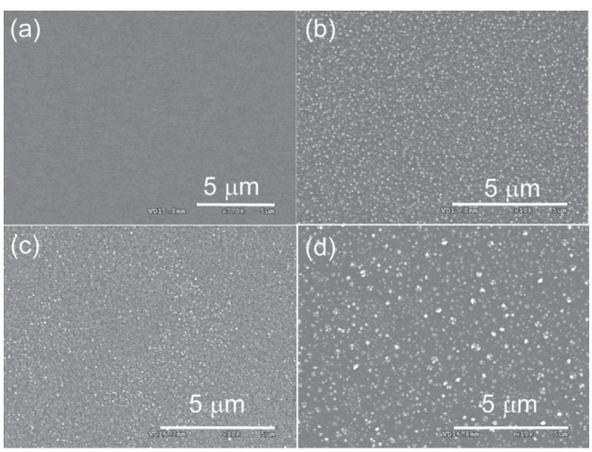

Fig. 2. SEM images of (a) Bare ITO; Au electrodeposited ITO surface for (b) −1.8, (c) −1.3 and (d) −0.13 V for 75 s.

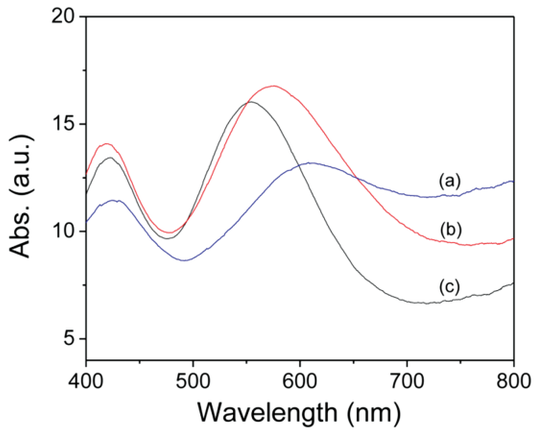

Fig. 3. UV visible spectroscopy of AuNPs/ITO substrate at different step potential (a) −1.8, (b) −1.3, and (c) −0.13 V.

and the inter particle distance reduction with higher particle density. The AuNPs size is a very important factor for the performance of enzyme electrode.

UV-vis spectra of the electrodeposited AuNPs are shown in Figure 3. The absorption spectra for the samples electrodeposited at −1.8 V, −1.3 V and −0.13 V showed the distinctive absorption peaks centered at 555, 576 and 608 nm, respectively (Figs. 3(a)–(c)), which can be attributed to the plasmonic absorption of electrodeposited gold nanoparticles. The difference in shape and size of the gold nanoparticles reflects in the absorption peak wavelength shift. The interparticle distance is also a prominent factor in plasmon absorption of such modified electrodes. A contact with the ITO substrates of high refractive index (−1.9 at ∼500 nm) which is known factor of red-shift in the resonance wavelength.[28] Even though it has been proved experimentally and theoretically that the extinction peak wavelength is red-shifted as the size of spherical particles increases, the smaller particles showed the more red-shifted peak than the larger particles.[28–29] This may be attributed to stronger plasmon coupling in the former because of the shorter interparticle distance.[30–31] The absorption peaks observed at 410–430 nm are probably due to residual interference fringes of the ITO film because of incomplete cancellation of the fringes.[28]

3.2. Electrochemical Behavior of Mb/AuNP/ITO Electrode

The characteristic CV responses were measured in N_2-saturated 10 mM PBS buffer (pH 7.0) at the scan rate of 100 mV s^{-1} to get the real surface information of the AuNPs electrodeposited ITO electrode. The scanning potential was varied from 0.5 to 0.0 V. Figure 4 shows the corresponding CV curves of (a) the bare ITO and (b) AuNPs/ITO electrodes. There is no observable faradaic current on the bare ITO electrode. A small increase in background current was observed for AuNPs/ITO electrode, which was due to the presence of AuNPs on ITO

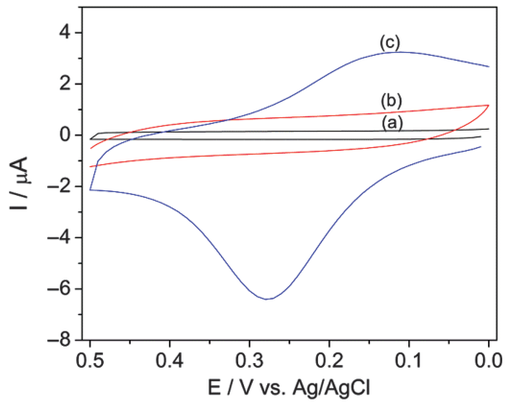

Fig. 4. Cyclic voltagrams of (a) bare ITO, (b) Au-ITO and (c)Mb/AuNPs/ITO electrode in 10 mM PBS, pH 7.0. Potential scan rate 0.1 mV s^{-1}.

surface resulted in generating the increased active electrode area. This gives another confirmation that the AuNPs are formed on ITO electrode surfaces. A pair of well-behaved and nearly symmetric redox peaks was observed at the Mb/AuNPs/ITO electrode. In contrast, there was no cathodic or anodic peak on both bare ITO (Fig. 4(a)) and AuNPs modified ITO (Fig. 4(b)) electrodes. It confirms clearly that the redox peaks of the Mb/AuNPs/ITO electrode are attributed to the direct electron transfer of redox protein Mb. The formal potential ($E_0 = (E_{pc} + E_{pa})/2$) was the active electrode was found to be 0.19 V.

Figure 5(a) depicts the typical CVs of the enzyme electrode in 10 mM PBS (pH 7.0) at different scan rates. With the increasing potential scan rate, a linear increase and shift in the separation of the anodic and cathodic peak potentials was observed. The anodic (I_{pa}) and cathodic (I_{pc}) peak currents are both linearly proportional to the scan rate from 10 to 100 mV s^{-1}, as displayed in the inset fo Figure 5(a). All these results are in agreement with the typical surface-controlled or thin-layer electrochemical behavior, as expected for immobilized systems.

3.3. Electrocatalytic Performance of Mb/AuNP/ITO for the Detection of H_2O_2

The potential 0.05 V was applied for determination of typical amperoemmetric response of Mb/AuNPs/ITO. The electrocatalytic properties of the Mb/AuNPs/ITO towards

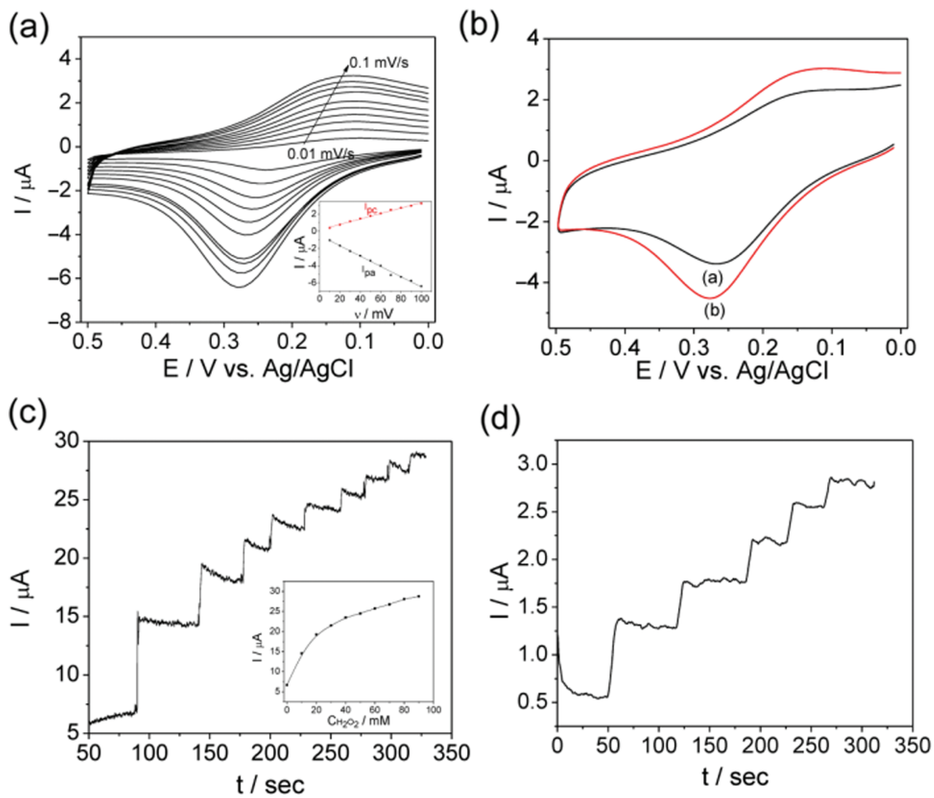

Fig. 5. (a) Cyclic voltagrams of Mb/AuNPs/ITO electrode with increasing scan rate from 0.01 to 0.1 mV s^{-1}; (Inset of (a) shows plot of cathodic (I_{pc}) and anodic (I_{pa}) peak currents versus scan rate.), (b) Cyclic voltagrams of Mb/AuNPs/ITO electrode in absence (black) and in presence (red) of 10 μL of 100 mM H_2O_2 in 10 mM PBS, pH 7.0 with increasing scan rate from 0.01 to 0.1 mV s^{-1} (c) Amperometric I–t curve obtained for (c) Mb/AuNPs/ITO, (d) AuNPs/ITO electrode upon successive addition of 10 μL aliquots of 100 mM H_2O_2 in 10 mL stirred 10 mM PBS at pH 7.0 with an applied potential of 0.05 V under nitrogen atmosphere. (c) inset shows plot of catalytic peak current versus H_2O_2 concentration.

H_2O_2 are shown in Figure 5(b). A stepwise increase in currents was observed after successive addition of 10 μL of 100 mM H_2O_2 to 10 mL of buffer solution. To confirm that the enhancement in current of sensor is from active element that is Mb, the amperometric response of AuNPs/ITO was also recorded (Fig. 5(d)). No significant enhancement in amperometric current was observed after addition of 10 μL of 100 mM H_2O_2. Hence the detection of H_2O_2 is purely caused from catalytic activity of Mb immobilized on AuNPs/ITO.

The electrocatalytic process can be expressed as follows:

$$\text{MbFe(III)} + e^- \rightarrow \text{MbFe(II)} \tag{1}$$

$$H_2O_2 + \text{MbFe(II)} \rightarrow 2\text{MbFe(III)} + 2H_2O \tag{2}$$

In the presence of H_2O_2, MbFe(II) was efficiently converted to its oxidized form, MbFe(III). Consequently, more MbFe(III) molecules were reduced at the electrode surface by the direct electron transfer.

4. CONCLUSIONS

The enhanced direct electron transfer from Mb to gold nanostructure modified ITO demonstrated here. The H_2O_2 biosensor was made by immobilizing Mb protein on biocompatible gold nanostructures on ITO electrode surface. The redox formal potential of Mb on AuNPs/ITO was obtained to be 0.19 V $\pm$ 0.01 V (vs. Ag/AgCl) at nanostructure AuNPs/ITO surface. The electrochemical CV experimental observation reveals stable confinement of Mb on AuNPs/ITO electrode and its catalytic role in H_2O_2 reduction. During H_2O_2 detection, the sensor exhibits a stable, sensitive and good response with retained biological activity of Mb. Thus this provides an efficient strategy and a new promising platform for the study of electron transfer of proteins and the development of biosensors.

Acknowledgments: This research was supported by the Nano/Bio Science and Technology Program (M10536090001-05N3609-00110) of the Ministry of Education, Science and Technology (MEST), by the National Research Foundation of Korea (NRF) grant funded by the Korea government (MEST) (2009-0080860), and by the Graduate School of Specialization for Biotechnology Program of the Ministry of Knowledge Economy (MKE).

References and Notes

1. T. Ruzgasa, E. Csoregib, J. Emneus, L. Gorton, and G. Marko-Varga, *Analytica Chemica Acta Eur. J.* 3306, 123 (**1996**).
2. D. Tang, R. Yuan, and Y. Chai, *Electroanal.* 18, 259 (**2006**).
3. N. Yamashiro, S. Uchida, Y. Satoh, and Y. Morishima, *J. Nucl. Sci. Technol.* 41, 890 (**2004**).
4. C. Matsubara, N. Kawamoto, and K. Takamura, *Analyst* 117, 1781 (**1992**).
5. A. K. Yagati, T. Lee, J. Min, and J.-W. Choi, *Bioelectrochemistry* 80, 169 (**2011**).
6. F. He, Y. Tang, M. Yu, S. Wang, Y. Li, and D. Zhu, *Adv. Funct. Mater.* 16, 91 (**2006**).
7. M. B. Frish, J. R. Morency, M. C. Laderer, R. T. Wainner, K. R. Parameswaran, W. J. Kessler, and M. A. Deuy, *Proc. SPIE Int. Soc. Opt. Eng.* Proc. 7680, 768006 (**1993**).
8. Z. Naal, J.-H. Park, S. Bernhard, J. P. Shapleigh, C. A. Batt, and H. D. Abrun, *Anal. Chem.* 74, 140 (**2002**).
9. J. Wang, K. S. Carmon, L. A. Luck, and I. I. Sunia, *Electrochem. Solid-St.* 8, 61 (**2005**).
10. H. Yao, N. Li, Y.-Li Wei, and J.-J. Zhu, *Sensors-Basel* 5, 278 (**2005**).
11. L. Wang, W. Mao, D. Ni, J. Di, Y. Wu, and Y. Tu, *Electrochem. Commun.* 676, 673 (**2006**).
12. Z. Guo, J. Chen, H. Liu, and C. Cha, *Anal. Chim. Acta* 607, 30 (**2008**).
13. K. Park, D. Kwon, and J. Kwak, *J. Nanosci. Nanotechnol.* 11, 4305 (**2011**).
14. Y. Qiao, G. Yang, F. Jian, Y. Qin, and L. Yang, *Sensor Actuat. B-Chem.* 141, 205 (**2009**).
15. Z. Guo, J. Chen, H. Liu, and C. Cha, *Anal. Chim. Acta* 30, 607, 30 (**2008**).
16. Y. Wang, W. Qian, Y. Tan, S. Ding, and H. Zhang, *Talanta* 72, 1134 (**2007**).
17. M. Urzúa, A. Leiva, F. J. Espinoza-Beltrán, X. Briones, C. Saldías, and M. Pino, *J. Nanosci. Nanotechnol.* 12, 8391 (**2012**).
18. J. Li, J. Yu, F. Zhao, and B. Zeng, *Anal. Chim. Acta* 33, 587 (**2007**).
19. A. Kaniyoor and S. Ramaprabhu, *J. Nanosci. Nanotechnol.* 12, 8323 (**2012**).
20. B. Ballarin, M. C. Cassani, C. Maccato, and A. Gasparotto, *Nanotechnology* 22, 275711 (**2011**).
21. A. Babaei, D. J. Garrett, and A. J. Downard, *Int. J. Electrochem. Sc.* 7, 3141 (**2012**).
22. L.-S. Duan, Q. Xu, F. Xie, and S.-F. Wang, *Int. J. Electrochem. Sc.* 3, 118 (**2008**).
23. S. Liu, Z. Dai, H. Chen, and H. Ju, *Biosens. Bioelectron.* 19, 963 (**2006**).
24. Y. Hong and H.-Y. Gu, *Microchim. Acta* 164, 141 (**2009**).
25. L. J. Ye and R. P. Baldwin, *Anal. Chem.* 60, 2263 (**1988**).
26. A. K. Yagati, T. Lee, J. Min, and J.-W. Choi, *Colloid. Surface B* 92, 161 (**2012**).
27. T. Lee, Y.-H. Chung, Q. Chen, W. A. El-Said, J. Min, and J.-W. Choi, *J. Nanosci. Nanotechnol.* 12, 4119 (**2012**).
28. N. Sakai, Y. Fujiwara, M. Arai, K. Yu, and T. Tatsuma, *J. Electroanal. Chem.* 628, 7 (**2009**).
29. X. Dai and R. G. Compton, *Anal. Sci.* 22, 567 (**2006**).
30. W. Rechberger, A. Honhenau, A. Leitner, J. R. Krenn, B. Lampercht, and F. R. Aussenegg, *Opt. Commun.* 220, 137 (**2003**).
31. S. K. Ghosh and T. Pal, *Chem. Rev.* 107, 4797 (**2007**).

Received: 22 July 2012. Accepted: 20 December 2012.